HAL
open science

Geometric Model of a Narrow Tilting CAR using Robotics formalism

Salim Maakaroun, Wisama Khalil, Maxime Gautier, Philippe Chevrel

To cite this version:

Salim Maakaroun, Wisama Khalil, Maxime Gautier, Philippe Chevrel. Geometric Model of a Narrow Tilting CAR using Robotics formalism. 15th International Conference on Methods and Models in Automation and Robotics, Aug 2010, Miedzyzdroje, Poland. paper 9011. hal-00484258

HAL Id: hal-00484258

https://hal.science/hal-00484258

Submitted on 18 May 2010

HAL is a multi-disciplinary open access archive for the deposit and dissemination of scientific research documents, whether they are published or not. The documents may come from teaching and research institutions in France or abroad, or from public or private research centers.

L'archive ouverte pluridisciplinaire **HAL**, est destinée au dépôt et à la diffusion de documents scientifiques de niveau recherche, publiés ou non, émanant des établissements d'enseignement et de recherche français ou étrangers, des laboratoires publics ou privés.

Geometric Model of a Narrow Tilting CAR using Robotics formalism

Salim Maakaroun *°, Wisama Khalil*, Maxime Gautier*, Philippe Chevrel*°
*Institut de Recherche en Communications et Cybernétiques de Nantes (IRCCyN)
Nantes, France
(firstname.lastname@irccyn.ec-nantes.fr)
° Ecole des Mines de Nantes, Département d'automatique-Productique
Nantes, France
(firstname.lastname@emn.fr)

***Abstract*—The use of an Electrical narrow tilting car instead of a large gasoline car should dramatically decrease traffic congestion, pollution and parking problem. The aim of this paper is to give a unique presentation of the geometric modeling issue of a new narrow tilting car. The modeling is based on the modified Denavit Hartenberg geometric description, which is commonly used in Robotics. Also, we describe the special Kinematic of the vehicle and give a method to analyze the tilting mechanism of it. Primarily experimental results on the validation of the geometrical model of a real tilting car are given**.

I. INTRODUCTION

The idea behind narrow tilting car research is to develop a narrow vehicle that seats two people in tandem [1], [2], [3]. This will reduce the size requirement of a vehicle and can be operated on reduced size lanes thereby increasing the effective capacity of highways. Moreover being an electrical car, it will provide an ecologic solution for pollution in the cities.

The aim of this paper is to present the geometric model of a specific narrow tilting car "Lumeneo Smera" [4] through the analysis of its tilting mechanism.

To model a complex system [5] in 3D motion, we use a systematic method of geometrical description, based on the modified Denavit Hartenberg parameterisation [6], [7] and. This description allows us to automatically calculate the symbolic expression of the geometric, kinematics and dynamic models by using a symbolic software package SYMORO+ [8]

This method is described in subsection 2.1 and applied on the car in subsection 2.2.

Then we analyse the tilting mechanism of the vehicle in section 3 by analysing all the loops and branches which constitute the geometrical model of the car. At the end, experimental results based on measured angles are shown to validate the geometric model of this car.

II. GEOMETRICAL DESCRIPTION OF THE TILTING CAR

A. Robotic representation of a multibody system

The car can be seen as a mobile robot which is a tree-structured multibody system composed of n bodies (links) where the chassis is the mobile base and the wheels are the terminal links. Each body C_j is connected to its antecedent C_i (i=a (j)) with a joint that represents a translational or rotational degree of freedom and can be elastic or rigid. A body can be virtual or real ; the virtual bodies are introduced to describe joints with multiple degrees of freedom like ball joint or intermediate fixed frames.

The frame R_i (O_i ,x_i , y_i , z_i) which is attached to the body C_i is defined as following:

The z_i axis is along the axis of joint i, the u_j axis is defined as the common normal between z_i and z_j. The x_i axis is along the common normal between z_i and one of the succeeding z axis, where link i is the antecedent of link j and the origin O_i is the intersection of z_i and x_i.

The homogeneous transformation ${}^iT_j$ of the frame R_i with respect to R_i is expressed as a function of the following six parameters (Fig. 1):

- γ_j: angle between x_i and u_j about z_i
- b_j: distance between x_i and u_j along z_i
- α_j: angle between z_i and z_j about u_j
- d_j: distance between z_i and z_j along u_j
- θ_j: angle between u_j and x_j about z_j
- r_j: distance between u_j and x_j along z_j

In (Fig.1), since x_i is taken along u_k, the parameters γ_k and b_k are equal to zero.

The generalized coordinate of joint j is denoted by q_j, and is equal to r_j if j is translational and θ_j if j is rotational.

We define the parameter $\sigma_j = 1$ if joint j is translational and $\sigma_j = 0$ if joint j is rotational. If there is no degree of freedom between two frames that are fixed with respect to each other, we take $\sigma_j = 2$.

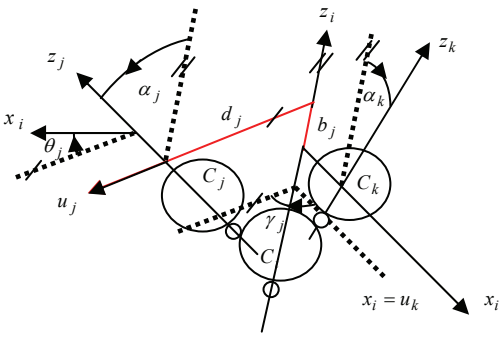

Figure 1. Geometric parameters

B. *Application for the car*

The model of the car is composed of 19 real bodies connected by 24 joints:

- B_1 is the chassis
- B_2 and B_9 are two mechanical parts called "lyre" which have a rotational movement around the longitudinal axis of the chassis. B_2 is actuated by an electrical motor which controls the roll of the vehicle.
- B_5 and B_8 are the rear wheels
- B_3, B_6 and B_{13}, B_{18} are respectively the rear and left dampers of the vehicle. They are considered as rigid springs to simplify the system
- B_4 and B_7 are the rear arms that connect the chassis to the rear wheels
- B_{14} and B_{19} are the front wheels
- B_{10}, B_{11}, B_{12} and the chassis constitute a parallelogram which carries the hub of the left front wheel
- B_{15}, B_{16}, B_{17} and the chassis constitute a parallelogram which carries the hub of the right front wheel

As shown in (Fig. 2), the model is symmetric with respect to the longitudinal plan of the vehicle.

In order to study the tilting mechanism of this vehicle, we have to analyse the movement of all the loops and branches which constitute the car.

The loops are defined as follows:

- LP1 is composed of B_1, B_2, B_3 and B_4,
- LP2 is composed of B_1, B_2, B_6 and B_7,
- LP3 is composed of B_1, B_4, B_5, B_7, B_8 and the ground,
- LP4 is the left parallelogram, it is composed of B_1, B_{10}, B_{11} and B_{12},
- LP5 is composed of B_1, B_9, B_{10} and B_{13},
- LP6 is the right parallelogram which is composed by B_1, B_{15}, B_{16} and B_{17},
- LP7 is composed of B_1, B_9, B_{15} and B_{18}.

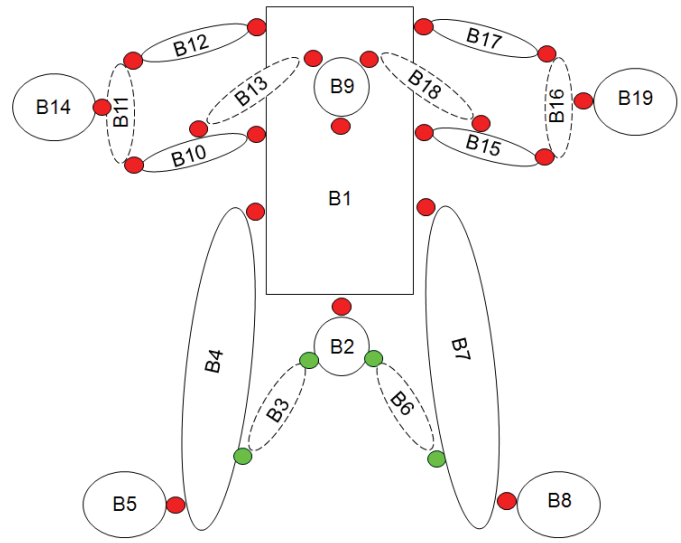

Figure 2. Description of the car

III. THE TILTING MECHANISM ANALYSIS

The principle of the tilting mechanism consists of a motor turning the back lyre and tilting the chassis which leads the front lyre.

We start our study by analyzing the loop LP1 and calculating the rotation angle of the left arm according to the motorized angle of the back lyre. Then we do the same analysis on the loop LP2 to calculate the rotation angle of the right arm. After that, we study the loop LP3 which connects the rear wheels of the vehicle to the chassis and the ground, where we calculate the tilt wheel angle according to the rotation angles of the left and right arms.

At this stage, we obtain the tilt angle of the wheels which is the tilt of the vehicle since the vertical plan constituted by the four wheels is always parallel to the vertical median plan of the chassis. At last, we analyze the four front loops LP4, LP5, LP6 and LP7 and we calculate all the rotation angles of all the joints that constitute these loops.

A. *Study of Loop Lp1*

This loop is formed by the back motorized lyre, the left rear damper, the left arm and the chassis. The top of the lyre is connected to the top of the damper by a spherical joint. Also the bottom of the damper is connected to the arm through a fixed fixture by a spherical joint. Finally the other end of the arm is linked to the chassis through a rotation around the axis of the left drive electrical engine. Thus we can conclude that this chain is a closed loop starting from the axis of the lyre up the axis of the drive engine, which is fixed to the chassis.

Let R_{01} be a fixed reference frame attached to the chassis; the model of this loop can be composed of 10 bodies C_j such that (Fig. 6):

- C_{0_1} is the base attached to the chassis and C_{10_1} is a virtual body used to define a second frame attached to the chassis,
- C_{1_1} is the motorized lyre
- $C_{2_1}, C_{3_1}, C_{5_1}, C_{6_1}$ and C_{7_1} are virtual bodies used to define the spherical joints.
- C_{4_1} is the damper
- C_{9_1} is the arm and C_{8_1} is a virtual body attached to the arm

We model this loop as a serial chain by imposing a constraint on the terminal frame depending on the position and orientation.

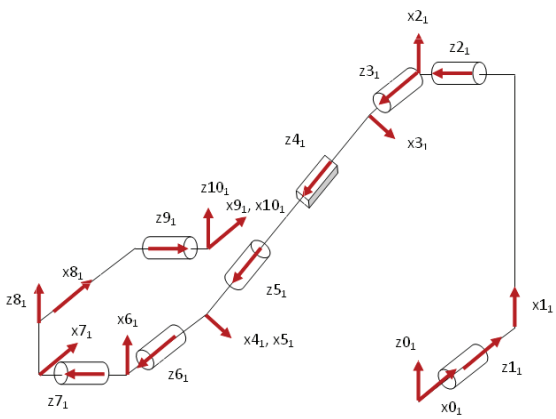

Figure 3. Description of loop LP1

TABLE I. GEOMETRIC PARAMETERS OF LOOP LP1

j	a(j)	σ_j	γ_j	b_j	α_j	d_j	θ_j	r_j
1_1	0_1	0	π/2	0	π/2	0	θ_{1_1}	0
2_1	1_1	0	0	0	π/2	L_1	θ_{2_1}	L_2
3_1	2_1	0	0	0	π/2	0	θ_{3_1}	0
4_1	3_1	1	0	0	π/2	0	0	r_4
5_1	4_1	0	0	0	0	0	θ_{5_1}	0
6_1	5_1	0	0	0	-π/2	0	θ_{6_1}	0
7_1	6_1	0	0	0	-π/2	0	θ_{7_1}	L_3
8_1	7_1	2	0	0	π/2	0	0	L_4
9_1	8_1	0	0	0	π/2	L_5	θ_{9_1}	L_6
10_1	9_1	2	0	0	-π/2	0	0	0

The imposed constraint on the terminal frame consists of fixing it to the chassis as the frame R_0. Thus these two frames move at the same time and in the same way when the vehicle tilts. The only difference is at the level of the position.

Therefore the resolution of the constraint equations corresponds to the resolution of the inverse geometric model IGM that gives all the robot configurations corresponding to a given location of the end effector.

The 4x4 homogenous transformation matrix ${}^{0_1}T_{1_1}$ between R_{0_1} and R_{10_1} is:

$$ {}^{0_1}T_{10_1} = \begin{bmatrix} 1 & 0 & 0 & P_x \\ 0 & 1 & 0 & P_y \\ 0 & 0 & 1 & P_z \\ 0 & 0 & 0 & 1 \end{bmatrix} \quad (1) $$

Where P_x, P_y and P_z are the position coordinate of the frame R_{101} with respect to the frame R_{01}.

This serial chain has one motorized joint θ_{1_1} and six passives joints $\theta_{2_1}, \theta_{3_1}, \theta_{4_1}, \theta_{6_1}, \theta_{7_1}$ and θ_{1_1}. Since there are three rotation joints of convergent axes, the maximum number of solutions must be 8 [9].

We apply the numerical algorithm in appendix A on this loop and we obtain 8 possible configurations. To visualize which of these solutions corresponds to the real configuration of the chain, we use Corke Robotics Toolbox [10] on Matlab to draw the solutions (Fig. 4).

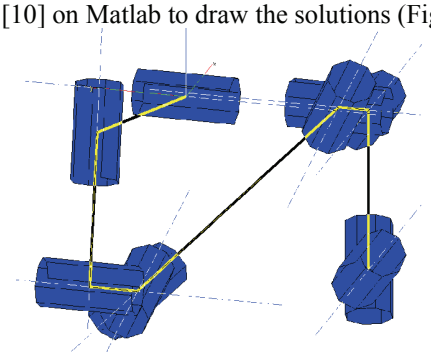

Figure 4. Simulation of a solution of LP1

B. *Study of loop LP2*

The architecture of this loop is the same as loop LP1 but in the opposite direction (fig.5). That means if the left arm goes up, then the right arms goes down due to the symmetric architecture of rear train.

We analyse this loop in the same way as loop LP1 to obtain at the end the rotation angle of the right arm.

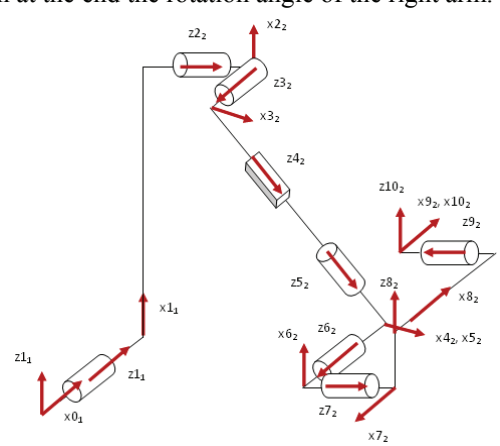

Figure 5. Description of loop LP2

TABLE II. GEOMETRIC PARAMETERS OF LOOP LP2

j	a(j)	σ_j	γ_j	b_j	α_j	d_j	θ_j	r_j
1_1	0_1	0	π/2	0	π/2	0	θ_{1_1}	0
2_2	1_1	0	0	0	-π/2	L_1	θ_{2_2}	L_2
3_2	2_2	0	0	0	-π/2	0	θ_{3_2}	0
4_2	3_2	1	0	0	π/2	0	0	r_4
5_2	4_2	0	0	0	0	0	θ_{52}	0
6_2	5_2	0	0	0	- π/2	0	θ_{6_2}	0
7_2	6_2	0	0	0	π/2	0	θ_{7_2}	L_3
8_2	7_2	2	0	0	π/2	0	0	L_4
9_2	8_2	0	0	0	-π/2	L_5	θ_{9_2}	L_6
10_2	9_2	2	0	0	π/2	0	0	0

TABLE III. GEOMETRIC PARAMETERS OF LOOP LP3

j	a(j)	σ_j	γ_j	b_j	α_j	d_j	θ_j	r_j
1_3	0_3	0	π/2	0	π/2	0	θ_{1_3}	0
2_3	1_3	2	0	0	π/2	0	π/2	R
3_3	2_3	0	0	0	π/2	0	θ_{3_3}	L_7
4_3	3_3	0	0	0	0	L_8	0	0
5_3	4_3	0	0	0	0	0	θ_{5_3}	L_9
6_3	5_3	0	0	0	0	L_8	θ_{6_3}	L_7
7_3	6_3	2	0	0	π/2	0	θ_{7_3}	-R
8_3	7_3	0	0	0	π/2	0	0	0
9_3	8_3	2	0	0	π/2	0	θ_{9_3}	0
10_3	9_3	2	0	0	π/2	0	0	0

C. *Study of loop LP3*

The left and right wheels, the left and right arms and the chassis form this loop. The entire joints between the bodies of this structure are rotational.

Let R_{03} be a fixed reference frame attached to the ground; the model of this loop can be composed of 10 bodies C_j such that (Fig. 6):

- C_{03} is the base attached to the ground and C_{9_3}, C_{10_3} are two virtual bodies used to define two frames attached to the ground
- C_{13} is the right wheel and C_{23} is a virtual body attached to it,
- C_{43} is the left arm and C_{33} is a virtual body fixed to the arm,
- C_{53} is the right arm and C_{63} is a virtual body attached to it,
- C_{83} is the left wheel and C_{73} is a virtual body attached to it.

The joints 1 and 8 represent the tilt of the wheels and consequently the tilt of the vehicle.

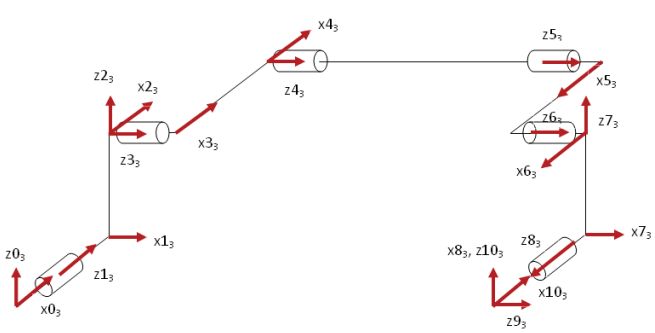

Figure 6. Description of loop LP3

We apply the algorithm in appendix A to this serial chain with the constraint equation between the frame R_{0_1} and R_{10_1}. As tires stay always in touch with the ground, we can say that P_z=0 and the error will be on $dX_c(:,3)$ and $dX_c(3,4)$.

For a given angle of the rotation of the back lyre, we resolve respectively loop1, loop2 and loop3 by making the necessary changes for the offsets of the joints between the different loops; thus we calculate the tilt of the vehicle.

The shape of the loop3 can be shown in figure (7) after applying an angle of rotation to the back lyre by using Corke robotics Toolbox (Fig. 7).

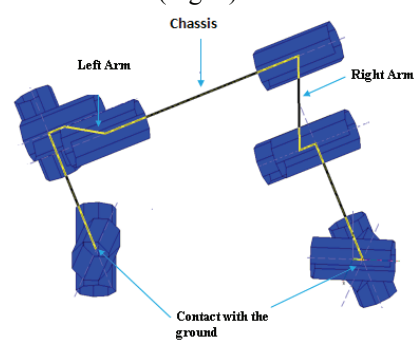

Figure 7. Simulation of loop LP3

Since the motion of all the front loops is planar, we will analyze analytically the geometric model of these loops. The principle of the analysis of closed loops consists on treating the equivalent tree structure that is obtained by cutting each closed loop at one of its joints and by adding two frames at each cut joint. The total number of frames is equal to n + 2B and the geometric parameters of the last B frames are constants. Thus, the position and orientation of all the links can be determined as a function of the active joint variables.

Loop Lp4 is at first analyzed in order to determine the relations between the various variables of the joints of this chain for a given tilt angle of the chassis.
Then we treat loop LP5, by considering shock absorbers also blocked as (section 3.1 and 3.2) and from the same given tilt angle, we calculate the rotation angle of the front lyre.
At this stage, we follow the reverse path across the lyre, by analysing loop7 corresponding to the calculated angle of the lyre in loop5.
At the end, the study of Loop 6 is similar to Loop 4.

D. *Study of loop LP4*

Let R_{04} be a fixed reference frame attached to the chassis; the model of this loop can be composed of 5 bodies C_j such that (Fig .8):

- C_{04} is the base attached to the chassis,
- C_{14} is the bottom arm of the left parallelogram
- C_{24} is the upper arm of the parallelogram
- C_{34} is always parallel to the chassis and caries the hub of the left wheel,
- C_{44} and C_{54} are two equal virtual bodies attached to C_{34} but with different antecedent

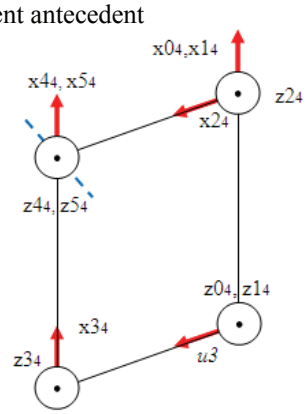

Figure 8. Description of loop LP4

TABLE IV. GEOMETRIC PARAMETERS OF LOOP LP4

j	a(j)	σ_j	γ_j	b_j	α_j	d_j	θ_j	r_j
1_4	0_4	0	0	0	0	0	θ_{1_4}	0
2_4	0_4	0	0	0	0	L10	θ_{2_4}	0
3_4	1_4	0	$\gamma 3_4$	0	0	L11	θ_{3_4}	0
4_4	2_4	0	0	0	0	L11	θ_{4_4}	0
5_4	2_4	2	0	0	0	L10	0	0

Let θ_{1_4} be the actuated joint of this loop and its value equal to the tilt of the vehicle. The symbolic resolution of the geometric constraint equations of Loop 4 is calculated by using a symbolic software SYMORO+ [7]:

$$\gamma_{3_4} + \theta_{1_4} + \theta_{3_4} - \theta_{2_4} - \theta_{4_4} = 0 \quad (2)$$

$$\theta_{1_4} + \theta_{2_4} = \gamma_{3_4} \quad (3)$$

$$\gamma_{3_4} + \theta_{1_4} + \theta_{3_4} = 0 \quad (4)$$

E. *Study of loop LP5*

Let R_{05} be a fixed reference frame attached to the chassis; the model of this loop can be composed of 5 bodies C_j such that (Fig. 9):

- C_{05} is the base attached to the chassis
- C_{15} is the front lyre
- C_{25} is the left blocked damper
- C_{35} is the bottom arm of the left parallelogram,
- C_{45} and C_{55} are two equal virtual bodies attached to C_{35} but with different antecedent

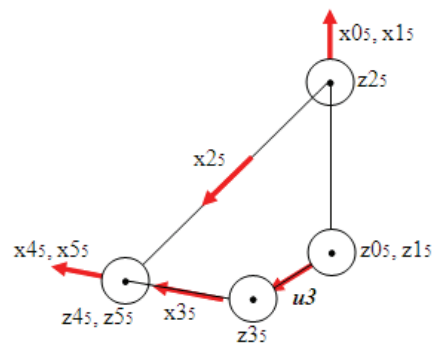

Figure 9. Description of loop LP5

The geometric parameters of loop LP5 are the same as loop LP4 with the following modifications:
$a(2_5)=1_5$; $a(3_5)=0_5$; $d_{25} = L_{12}$; $d_{35} = L_{15}$; $d_{45} = L_{13}$; $d_{55} = L_{13}$

Let $\theta_{3_5} = \theta_{1_4} + off$ be the actuated joint of this loop. The geometric constraint equations of Loop LP5 are given by using SYMORO+:

$$\gamma_{3_5} - \theta_{15} - \theta_{2_5} + \theta_{3_5} - \theta_{45} = 0 \quad (5)$$

$$\theta_{2_5} = \pm a\cos\left(\frac{-L_{12}^2 - L_{13}^2 + L_{15}^2 + L_{14}^2 + 2L_{14}L_{15}\cos\theta_{3_5}}{2L_{12}L_{13}}\right) \quad (6)$$

$$L_{15} + L_{14}\cos\theta_{3_5} - L_{13}\cos\theta_{4_5} - L_{12}\cos(\theta_{2_5} + \theta_{4_5}) = 0 \quad (7)$$

$$-L_{14}\sin\theta_{3_5} + L_{13}\sin\theta_{4_5} + L_{12}\sin(\theta_{2_5} + \theta_{4_5}) = 0 \quad (8)$$

Since the architecture of the loop, we select the positive value of equation (6). θ_{45} is calculated from (7) and (8) :

$$\theta_{4_5} = a\tan(\sin(\theta_{4_5}), \cos(\theta_{45})) \quad (9)$$

Where

$$\sin\theta_{4_5} = \frac{(L_{13} + L_{12}\cos\theta_{2_5})(L_{14}\sin\theta_{3_5}) - L_{12}\sin\theta_{2_5}(L_{15} + L_{14}\cos\theta_{3_5})}{L_{13}^2 + L_{12}^2 + 2L_{13}L_{12}\cos\theta_{2_5}}$$

$$\cos\theta_{4_5} = \frac{(L_{13} + L_{12}\cos\theta_{25})(L_{15} + L_{14}\cos\theta_{3_5}) + L_{12}\sin\theta_2 L_{14}\sin\theta_3}{L_{13}^2 + L_{12}^2 + 2L_{12}L_{13}\cos\theta_{2_5}}$$

At the end, θ_{15} is calculated by (5).

F. Study of loop LP6 and LP7

The analysis of LP6 and LP7 is respectively the same as LP4 and LP5 with these modifications:
-we study LP7 before LP6,
-the actuated joint of LP7 is θ_{17} and is equal to θ_{15} calculated in (5),
-the actuated joint of LP6 is θ_{16} and is equal to θ_{37} $+off$ calculated in LP7.

IV. Experimental results

Primarily experimental results are given. For the data acquisition, a real tilting car is equipped with many sensors which allow the validation of the geometrical model.
Those sensors are: a position sensor, 3 gyroscopes and 3 accelerometers. They allow us to specify the rotation angle of the front lyre and the tilt of the vehicle.

A. Results

TABLE V. Experimental results

TEST	1	2	3	4	5	6	7
RLD(m)	0.275	0.272	0.2685	0.275	0.275	0.275	0.275
RRD(m)	0.278	0.278	0.2765	0.274	0.267	0.267	0.277
FLD(m)	0.278	0.275	0.2695	0.28	0.2785	0.276	0.28
FRD(m)	0.280	0.279	0.278	0.28	0.2735	0.268	0.28
CTA(°)	6.875	12.03	18.793	-5.32	-16.61	-20.5	1.4
CFL(°)	6.92	11.68	17.24	-6.12	-16.9	-18.5	0.114
ETA(°)	6.875	12.03	18.79	-5.32	-16.61	-20.5	0
MFL(°)	6.75	10.89	15.98	-5.7	-15.38	-18.0	0

Where:
RLD, RRD, FLD and FRD are respectively the rear left and right dampers and the front left and right dampers;
CTA and CFL are respectively the calculated tilt angle and the calculated front lyre angle;
ETA and MFL are respectively the estimated tilt angle and the measured front lyre angle. The ETA is obtained from the accelerometers with the aim of cancelling the effect of the centrifugal force.
By comparing the measured or estimated angles and the calculated angles, we conclude that margin of error is between [0°, 2°]. Therefore the geometric model is validated.

V. Conclusions

Despite the validation of the geometric model, it is important to notice that all tests have been realized with blocked dampers and this case does not reflect the reality. Therefore we have to consider later the elasticity of the dampers in order to calculate the dynamic model of the vehicle, to identify the dynamic parameters and finally to simulate the behaviour of the car. Future work will concern the identification of the dynamic parameters and the control of the lyre angle to ensure the stability of the vehicle.

References

[1] Gohl J., Rajamani R. and al , Development of a Novel Tilt-Controlled Narrow Commuter Vehicle, (internal report) May 2006.

[2] So SG., Karnopp D Active dual mode tilt control for narrow ground vehicle, *Vehicle System Dynamics journal*, vol 27, pp19-36 1997.

[3] Hibbard R., Karnopp D, the dynamics of small, relatively tall and narrow tilting ground vehicle, *ASME Dynamics Systems and Control*, 52, pp. 397-417 1992.

[4] Lumeneo, www.lumeneo.fr

[5] Rajamani R., *vehicle dynamics and control*, Springer 2005

[6] Khalil W., Kleinfinger J.F., A new geometric notation for open and closed loop robots, *Proc. IEEE on robotics and automation*, pp. 1174- 1180, San Francisco, CA, USA 1986.

[7] Khalil W., Creusot D, SYMORO+: a system for the symbolic modelling of robots, *Robotica*, Vol. 15, 1997, p. 153-161 1997.

[8] Pieper D. (1968), The kinematics of manipulators under computer control , PhD Thesis, Stanford University, UK 1968.

[9] Corke P.., A Robotics Toolbox for MATLAB, *IEEE on robotics and automation, N01,* pp. 24-32-, vol 3 1996.

[10] Khalil W. and Dombre E. , *Modelling, identification and control of robots*, Hermès Penton, London & Paris 2002 .

Appendix A: Numerical calculation of the inverse geometric model

When it is not possible to find an explicit form to the inverse geometric model, we can use the Kinematic model to calculate recursively numerical solution q^{d} corresponding to a desired situation ${}^{0}T^{d}{}_{n}$. The algorithm is defined as:

-Define an initial random configuration q^{c} ,

-Calculate the direct geometrical model ${}^{0}T^{c}{}_{n}$ corresponding to this configuration,

-Calculate the error $dX_c = \left[dX_p^T \quad dX_r^T\right]^T$ between ${}^{0}T^{d}{}_{n}$ and ${}^{0}T^{c}{}_{n}$, where $dX_p = P_n^d - P_n^c$ and $dX_r = u\alpha$

- Define a threshold S to dX_c:

If $\|dX_c\| > S$ then, $dX_c = \dfrac{dX_c}{\|dX_c\|} S$

Else Stop the calculation and q^{d} will be equal to q^{c} .

-Calculate numerically the direct Jacobian matrix ${}^{0}J_n(q_c)$ and her pseudo-inverse J^{+},

-Calculate $dq = J^{+} dX$ then update the current configuration: $q^{c} = q^{c} + dq$ and return to the second step.

We notice that if the algorithm does not converge after a predefined number of iterations, or if we need to obtain another different solution, it is necessary to begin again the calculation with a new initial value.